Eur Biophys J (2012) 41:241–248
DOI 10.1007/s00249-011-0779-z

ORIGINAL PAPER

EBSA
Biophysics in Europe

Docking and molecular dynamics simulation studies on glycation-induced conformational changes of human paraoxonase 1

Ammara Saleem · S. Sikander Azam · Shamshad Zarina

Received: 17 September 2011 / Revised: 19 November 2011 / Accepted: 22 November 2011 / Published online: 23 December 2011

Abstract Human paraoxonase 1 (huPON1) is a calcium-dependent esterase responsible for hydrolysis of a wide variety of substrates including organophosphates, esters, lactones, and paraoxon. Although its natural substrate is unknown, the action of PON as an antioxidant is well documented. Because recent reports have suggested glycation may induce reduced PON activity in diabetes, we investigated the structural features of huPON1 and its glycated mutant by template-based modeling, docking, and molecular dynamics (MD) simulations. Our results corroborated the importance of the His115–His134 dyad in both the lactonase and paraoxonase activity of huPON1. Structural alterations in the glycated model reflected weak interactions between the docked substrate and the active site cleft. We also used MD simulation to gain insight into glycation-induced conformational changes of huPON1 and the implication of this on depleted enzymatic activity. The catalytic calcium found on the surface interacts with the side chain oxygen of residues, including Asn224, Asn270, Asn168, Asp269, and Glu53, and this interaction with the respective residues undergoes minor displacement on glycation. The root-mean-square fluctuation had high motional flexibility in the non-glycated model whereas the conformation of the glycated structure was comparatively stable. Our findings emphasize the consequence of glycation-induced alterations and their effect on overall enzymatic activity.

Keywords Human paraoxonase 1 · Paraoxon · Lactones · Molecular dynamics · Glycation · Structure prediction

A. Saleem · S. S. Azam · S. Zarina (✉)
National Center for Proteomics, University of Karachi, Karachi 75270, Pakistan
e-mail: szarina@uok.edu.pk

Present Address:
S. S. Azam
National Center for Bioinformatics, Quaid-i-Azam University, Islamabad, Pakistan

Introduction

Human paraoxonase 1 (huPON1) is a calcium-dependent esterase located on chromosome 7. It belongs to a multigene family containing three members, PON1, PON2, and PON3 (Primo-Parmo et al. 1996). Although all three members share 65% homology at the sequence level, they differ in their expression pattern. PON1 and PON3 are primarily expressed in the liver and are circulated in the blood in association with high-density lipoproteins (HDL) whereas PON2 is ubiquitously expressed in a variety of tissues except blood (Mackness 1989; Reddy et al. 2001). The natural substrate, and hence the physiological action of this family is unknown. The most extensively studied member of the group, PON1 has paraoxonase, arylesterase, and lactonase activity and is capable of neutralizing toxic compounds, for example xenobiotics (Shih et al. 1998; Davies et al. 1996; Broomfield and Ford 1991; Billecke et al. 2000). PONs have a protective effect against LDL oxidation, thus reducing levels of cholesterol (Ng et al. 2001), indicating their antiatherogenic property (Liu et al. 2008). Animal model studies have proved that PON expression is capable of inhibiting or reverting atherosclerosis development by reducing oxidative stress, thus acting as an anti-oxidant (Shih et al. 1998). Reduced PON1 activity has been reported in many disorders, including cancers, Alzheimer's disease, cardiovascular diseases, diabetes, and cataract which is not unexpected, because

oxidative imbalance has been implicated in etiology of these disorders (Upham and Wagner 2001; Dhalla et al. 2000; Vinson 2006; Hashim and Zarina 2007). It has also been suggested that oxidative stress is a consequence of hyperglycemia, because of the possibility of glucose autooxidation and generation of advanced glycation end products (AGEs) (Baynes and Thorpe 1999). Indeed, loss of PON1 activity has been found to be greater in diabetic subjects than in controls (Hashim and Zarina 2007).

Human PON1 (huPON1) contains 355 amino acid residues, and its catalytic site, binding interactions with HDL, and antioxidant capability at a structural level have been studied in detail (Harel et al. 2004). The crystal coordinates of PON1 available at the Protein Databank are of recombinant PON, which has a characteristic six bladed β propeller structure having two calcium ions for the stability and catalytic activity of the protein (Harel et al. 2004). One of the calcium ions (Ca1), the catalytic calcium, is found on surface whereas the other calcium ion (Ca2) has a structural role and is located in the central region. The calcium ions are approximately 3 Å apart (Kuo and La Du 1998). Ca1 interacts with the side-chain oxygen of five residues including Asn224, Asn270, Asn168, Asp269, and Glu53, and with water molecules and the oxygen of phosphate ions (Kuo and La Du 1995). The catalytic calcium facilitates formation of the enzyme–substrate complex and accelerates the breakdown of intermediates into enzyme and products (Eckerson et al. 1982). The residues found to be crucial for huPON1 activity include Lys70, Tyr71, Leu240, Val346, Phe292, Ile291, Phe222, Leu69, His115, His134, His285, Thr332, Leu267, and Phe347 (Harel et al. 2004; Josse et al. 2001). Among these, it has been suggested that the His115–His134 dyad is catalytically important for lactonase activity (Khersonsky and Tawfik 2006). There is no direct evidence indicating involvement of His115 in paraoxonase activity. A recent study has revealed the importance of Tyr71, Pro72, Arg192, Leu191, Met196, Asp188, Pro189, Phe222 and Phe292 to paraoxonase activity (Hu et al. 2009).

Structural analysis of protein models using MD simulations has recently generated much interest among computational biologists. The objective of this study was to evaluate the effect of glycation on the binding capability of huPON1 after docking of the substrates paraoxon and lactones into the active site. To examine glycation-induced conformational variations, MD simulation studies of huPON1 with and without glycation on the picosecond time scale have also been conducted. To the best of our knowledge, this is the first attempt to examine structural variation of the huPON1 glycated model using MD simulation.

Methods and materials

Computational resources

Bioinformatics analysis of protein molecules was performed on Sun Ultra 20 M2 work stations under licensed Windows XP and the models were constructed using Modeller 8v1 (Sali and Blundell 1993). The docking study was performed using FlexX version 3.1.1 (Rarey et al. 1996) and visual inference was carried out using Chimera (Pettersen et al. 2004) and Discovery Studio Visualizer. MD simulations were carried out on an AMD opteron Model 2220 dual core (1.8 GHz) equipped with a Linux environment running under Redhat 5.1. Amber 10 (Case et al. 2008) was used for MD simulation and VMD (Humphrey et al. 1996) was used for visualization of trajectories.

Modeling of human paraoxonase 3D structure

The glycated and non-glycated models of huPON1 were constructed as described elsewhere (Hashim et al. 2009). In brief, the amino acid sequence of huPON1 (Acc. no: P27169) was retrieved from UniProtKB/Swiss-Prot database (Bairoch and Apweiler 1996) and was subjected to the BLAST (basic local alignment search tool) algorithm (Altschul et al. 1997) against PDB. The target sequence was 84% identical (92% similarity) with the recombinant paraoxonase structure (PDB ID: 1V04) with an E-value of 0.0. The three-dimensional structure of huPON1 was constructed using crystal structure coordinates (resolution: 2.2 Å) of recombinant paraoxonase 1V04 using Modeller (Sali and Blundell 1993). Modeller is a completely automated program capable of generating energy-minimized models using CHARMM as energy-minimization tool. Twenty models of huPON1 were constructed and the best was selected after evaluation by Procheck (Laskowski et al. 1993). All models (normal and mutated) were evaluated by use of ProSa (Wiederstein and Sippl 2007). For creation of glycated mutants, potential glycation sites were predicted using the NetGlycate 1.0 Server; (http://www.cbs.dtu.dk/services/NetGlycate/) which identified 13 Lys residues which could possibly be glycated. Glycated mutants were created as described elsewhere (Hashim et al., 2009). Briefly, pentosidine, and carboxymethyllysine were inserted at Lys70 and Lys75 using the molecular graphic software Discovery Studio Visualizer. Further, the models were equilibrated and energy-minimized by use of Chimera software (Pettersen et al. 2004). After minimization the protein molecules were docked with different ligands.

Docking studies

Lactones and paraoxon were docked on glycated and non-glycated models of huPON1 by use of FlexX (Rarey et al. 1996). The mol2 files of ligands were obtained from the Pubcomp library of the NCBI database (http://www.ncbi.nlm.nih.gov/pccompound). FlexX uses the incremental construction algorithm and optimizes the torsion angles of the ligand without altering its bond length and angles. Essential residues for PON1 activity within a range of 10 Å radius were included in the cavity binding the ligand (Harel et al. 2004) during the analysis. Default values and the SIS algorithm of FlexX were used for this work. The software generates more than 100 poses which are numbered according to the minimum docking energies calculated by use of a built-in scoring function. FlexX docking interactions were visualized by use of LigPlot (Wallace et al. 1995).

Molecular dynamics (MD) simulations

MD simulations were carried out for glycated (pentosidine) and non-glycated PON1 in an explicit solvent system using Amber (Case et al. 2008) and the force field 03 (Ryckaert et al. 1977). To maintain the neutrality of the system, 11 and 16 Na^+ ions were added in glycated and non-glycated huPON1, respectively. The models were solvated by 4,185 and 3,434 water molecules, respectively, in a rectangular box around the solute unit. The sizes of the cells were 100.59 Å × 118.34 Å × 117.32 Å, consisting 72,145 atoms, and 98.62 Å × 94.43 Å × 107.53 Å, consisting 32,528 atoms, for glycated and non-glycated huPON1, respectively. The rectangular solvation box was created by using the Xleap interface of Leap. The solvated protein systems were subjected to a thorough energy minimization before undergoing MD simulations. To relax the system and to avoid any steric conflicts, minimization of water molecules was conducted while holding the solute fixed (1,000 steps using the steep descent algorithm followed by 1,000 steps of conjugate gradient minimization of the whole system). Bond lengths involving hydrogen were constrained with the SHAKE algorithm (Berendsen et al. 1984). The time step for all MD simulations was set to 2 fs, a nonbonded cutoff of 8 Å was used, and periodic boundary conditions were used to simulate a continuous system. The system was then subjected to a gradual temperature increase from 0 to 300 K over 100 ps, and then equilibrated for over 100 ps at 300 K, followed by the production run of 5 ns. Temperature (298 K) and pressure (1 atm) were kept constant by using the Berendsen coupling algorithm with a time constant for heat-bath coupling of 0.2 ps. The dielectric constant was set to 1.0. Long-range electrostatic calculations were performed by the particle mesh Ewald method. The resulting trajectories were analyzed by the use of PTRAJ module of the Amber package.

Results

Glycated and non-glycated models of huPON1

After construction of the huPON1 model using 1V04 as a template, the best model was selected on the basis of stereochemical properties as evaluated by Procheck. The Ramachandaran plot revealed 99.2 and 0% residues in the most favored and disallowed regions, respectively. For glycation, Lys 70 and 75 were selected as potential glycation site, because both residues are located on the active site lid and are of critical importance in movement of the active site lid and substrate entry. Models of glycated (pentosidine and carboxymethyllysine) huPON1 were constructed and the best models were selected on the basis of their Ramachandaran plot (99% residues in the most favored region). None of the residues were found in the disallowed region. All structures were validated by use of ProSa, which gave Z scores of −6.83 and −7.29 for the template 1V04 and all huPON1 models (glycated and non-glycated), respectively.

Docking studies

The glycated and non-glycated models of huPON1 were docked individually with 14 lactones, paraoxon, mioticol, and nitrophenylhalon. Each ligand was docked deep into the active site of mutated and normal protein molecules, and best interactions were selected on the basis of docking energies. A remarkable increase was noticed in docking energies in glycated protein models compared with the non-glycated protein (Table 1). This variation was found to be more for the pentosidine adduct than for that of carboxymethyllysine, so we focused on the pentosidine adduct for further analysis. All results shown for the glycated mutant refer to the pentosidine adduct unless stated otherwise. Figure 1a, b shows the interaction of the glycated and non-glycated models of huPON1 with that of dihydrocoumarin (lactone). Fig. 2a, b depicts the docked conformation of huPON1 (pentosidine adduct and non-glycated) with paraoxon.

Molecular dynamics simulation

After observing deviations in the interaction of the substrate with the glycated and non-glycated models of huPON1, we tried to compare the dynamics of these structures using the MD simulation approach. For this purpose, the total energy of the whole system and the root-

Table 1 Docking energies of substrate interaction with glycated (pentosidine and carboxymethyllysine) and non-glycated models of huPON1

Substrate (lactones and paraoxon)	Docking energy (kJ/mol)		
	Non-glycated model normal	Glycated model (pentosidine)	Glycated model (carboxymethyllysine)
Dihydrocoumarin	−17.603	−11.691	−14.761
Coumarin	−16.121	−10.311	−14.2880
Gamma-butyrolactone	−11.603	−7.702	−8.7920
Gamma valerolactone	−11.210	−7.776	−5.9332
Gamma-hexalactone	−11.470	−6.197	−10.4981
Gamma heptalactone	−6.112	−6.156	−9.3496
Gamma-octalactone	−10.546	−6.006	−7.0069
Gamma nonalactone	−10.364	−4.671	−7.9157
Gamma-decalactone	−9.438	−4.462	−6.4252
Propiolactone	−10.710	−6.858	−9.9081
Pantolactone	−15.874	−12.936	−15.5164
Glucuronolactone	−15.391	−11.308	−19.7143
Paraoxon	−4.9533	−2.0644	−4.9533
Mioticol (Diisopropyl paraoxon)	−0.6884	−1.2200	−0.6884
Nitrophenylhalon (2-Chloroethyl paraoxon)	−1.8597	0.9690	−1.8597

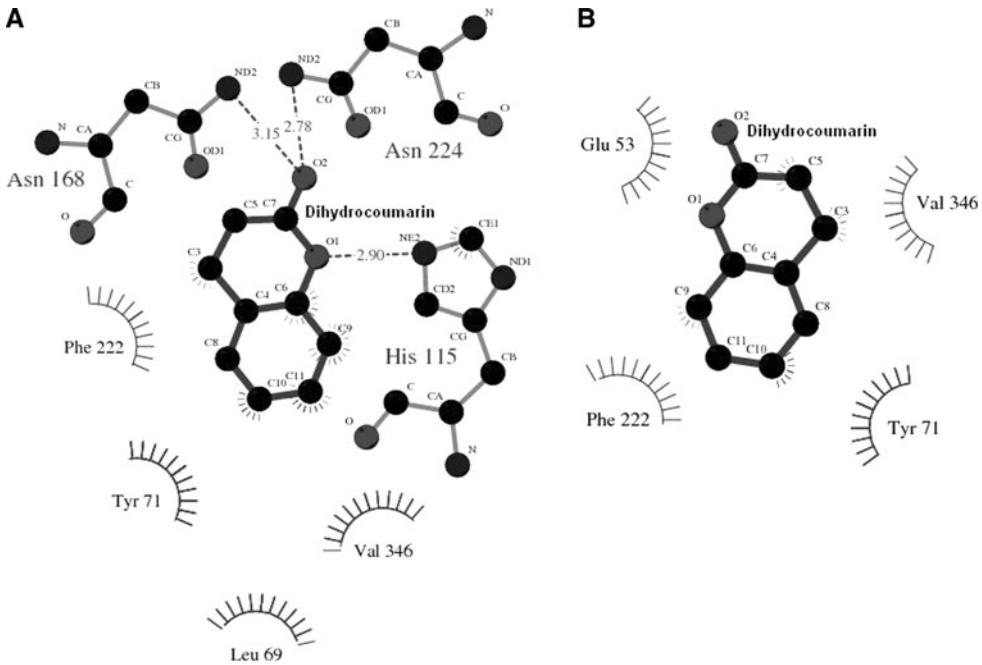

Fig. 1 Docked conformation of dihydrocoumarin with the non-glycated (**a**) and pentosidine-glycated (**b**) models of huPON1 using FlexX showing the interaction with the crucial residues in the active site cleft

mean-square deviation (RMSD) from the initial structure were observed to determine the sustainability and convergence of MD simulations. These changes in the structural conformation were monitored in terms of RMSD and root-mean-square fluctuations (RMSF). Figure 3 shows plots of RMSDs calculated for the backbone atoms of the two simulated systems over the entire simulation of 5 ns. Figure 4 shows RMSF plots of glycated huPON1 and non-glycated huPON1 with average values of 4.24 Å and 4.38 Å, respectively.

Discussion

Contemporary developments in computational approaches, for example docking studies and molecular dynamics simulation methods, have led to new means of investigation of the interactions between a protein molecule and its substrate (Azam et al. 2009; Lu et al. 2010). These tools are not only beneficial for identification of structural variations because of alteration of a single amino acid residue but also have the ability to find the orientation that participates in a

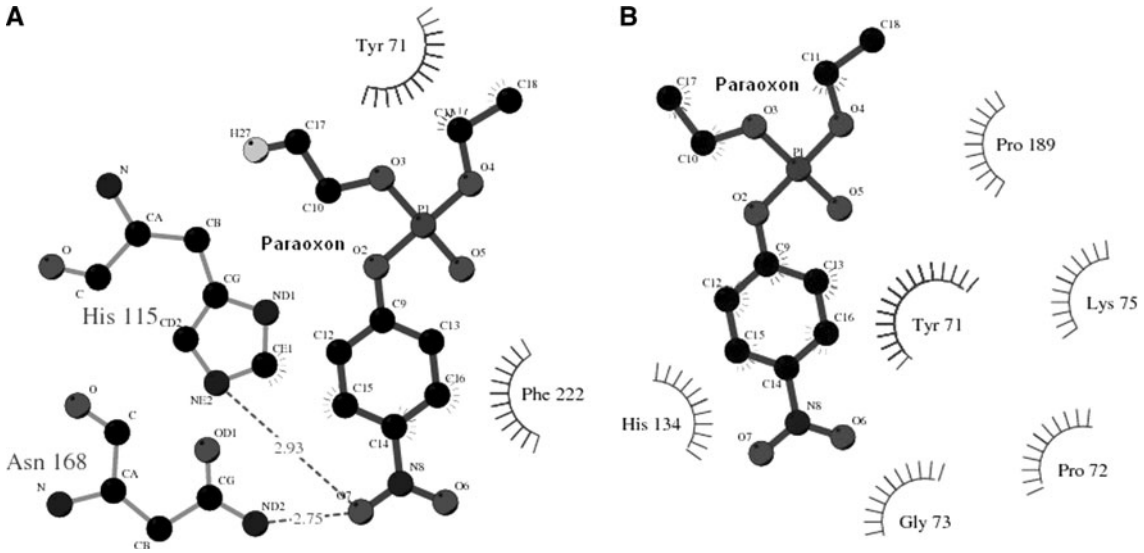

Fig. 2 Docking output of paraoxon with the non-glycated (**a**) and pentosidine-glycated (**b**) models of huPON1 showing the interaction of paraoxon

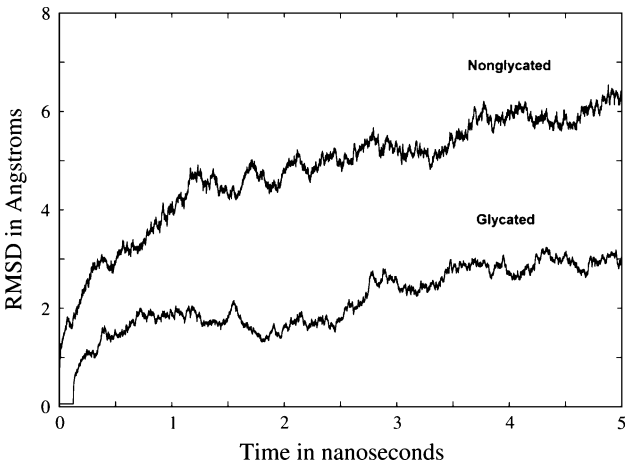

Fig. 3 Root-mean-square deviation (RMSD) of the Cα backbone for both non-glycated and pentosidine added models of huPON1 against the entire simulation of 5 ns

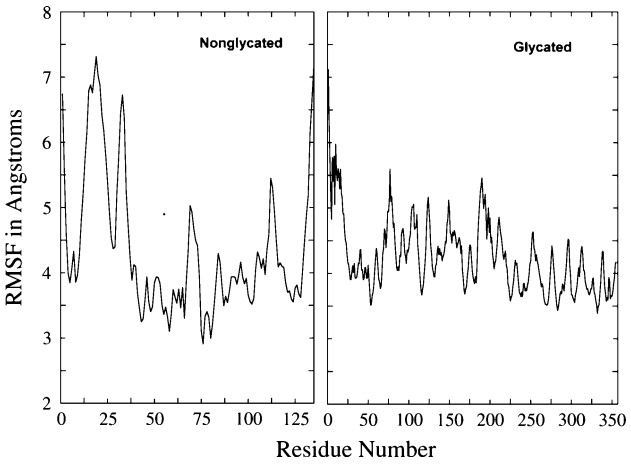

Fig. 4 Root-mean-square fluctuation (RMSF) of the Cα backbone of non-glycated (active site cleft) and pentosidine-glycated (whole protein) models

stable interaction having minimized energy (Gohlke et al. 2000; Kramer et al. 1999). In this study we focused on structural alterations of huPON1 induced by glycation after docking with lactones and paraoxon, because the enzymatic activity of huPON1 has been shown to be reduced by 40% on in-vitro glycation (Hedrick et al. 2000). Furthermore, MD simulation studies were performed to depict the interaction of molecules on the picoseconds time scale.

Docking of glycated and non-glycated huPON1 with lactones

Previous investigations have revealed that the His115–His134 dyad and Asp269, Asn168, and Asn224 are crucial for lactonase activity (Khersonsky and Tawfik 2006). Our docking analysis with lactones confirmed these interactions (Fig. 1a). In the glycated model, however, we observed that His115 is no longer involved in interaction with the substrate (Fig. 1b). Although some interactions (Tyr71 and Phe222) were retained in the glycated mutant, other interactions were found to be absent. Hydrophobic interactions of the glycated model with Glu53 and Val346, but not with Tyr71 and Phe222, were also observed. A recent study has revealed the involvement of Tyr71 in binding of the substrate with the active site (Hu et al. 2009). It is interesting to note that the Tyr71 interaction is retained in the glycated model. In the non-glycated model (Fig. 1a) hydrogen bond formation between His115, Asn168, and

Asn224 and the lactone (dihydrocoumarin) was also observed. The oxygen (O1) atom of dihydrocoumarin interacts with NE2 nitrogen of His115 (2.90 Å), and the oxygen O2 of dihydrocoumarin participates in hydrogen bonding with ND2 of Asn168 (3.15 Å) and Asn224 (2.78 Å). No hydrogen bonding was observed for the glycated mutant (Fig. 1b), indicating destabilization of active site cleft.

Docking of glycated and non-glycated huPON1 with paraoxon

The mechanism of hydrolysis of paraoxon by protein paraoxonase is unknown. Glycated and non-glycated huPON1 were docked with paraoxon, mioticol, and nitrophenylhalon. The resulting models revealed hydrogen bonding of His115 with all three molecules. The NE2 of His115 interacted with O7 (2.93 Å) of paraoxon, and ND2 of Asn168 formed a hydrogen bond with O7 (2.75 Å) of paraoxon. Tyr71 and Phe222 participated in hydrophobic interactions with paraoxon, as shown in Fig. 2a. More conformational changes in crucial residues were observed for the glycated model; these resulted in weak substrate–enzyme interaction (Fig. 2b). Normally, His134 provides the proton shuttle mechanism and supports the activity of His115. Because of the glycation, His134 and the active site lid residues, including Tyr71, Pro72, Gly73, and Lys75, interacted hydrophobically with the ligand molecule.

Simulation studies

The comparative evaluation of the two models was based on the RMSD and RMSF values obtained after simulation analysis. The average RMSD was less than approximately 2.12 Å for glycated huPON1. For the non-glycated huPON1, on the other hand, the RMSD was higher (approx. 4.79 Å) with an increasing trend (Fig. 3). This results mostly from the higher flexibility of the non-glycated system, which, on formation of the advanced glycation end products, is a comparatively stable conformation throughout the MD simulation. Recently reported RMSDs for non-glycated human PON (Hu et al. 2009) seem to be in agreement with our results.

Dynamic root-mean-square fluctuations (RMSF) of proteins around their average conformations are an important indicator of many biological processes, e.g. enzymatic activity. RMSF for our system of interest were examined for the C-alpha atoms of each residue, and represent the average displacements of these atoms. Figure 4 shows the fluctuations resulting from truncated PDB for the non-glycated model, whereas the whole protein was taken into account for MD simulation of glycated huPON1. Despite these higher values, the atomic fluctuations are slightly lower for glycated huPON1 suggesting that average RMSF decreases on formation of AGEs. This decrease in value is indicative of some hindrance in the enzymatic activity of the protein on glycation. This finding is in complete agreement with the outcome of our docking results. Because the X-ray structure of the glycated protein was not available, the RMSF value could not be compared.

Significant fluctuation within the regions surrounding the active site was observed for the non-glycated huPON1 compared with glycated huPON1, the overall fluctuation of which shows the stability of the system towards the end of simulation. The active site seems to deviate structurally for the non-glycated huPON1 model compared with the glycated one. Some flexibility was observed in the conformation of the catalytic His115, as was also observed in docking studies. After glycation, fluctuation and deviation were observed at Tyr71 and Lys70, which are important in recognition of the substrate and provide the backbone for the stability of the active site (Liu et al. 2008). Figure 5a, b shows the conformational changes brought about in the structure of non-glycated and glycated huPON1 at regular time intervals of 0, 3, and 5 ns, respectively. Because huPON1 is a calcium-dependent esterase, we also examined the role of calcium. Interaction of calcium with the five protein residues Asn224, His115, Asn168, Asp 269, and Glu53 seemed to be highly disturbed in the glycated model. Previous studies showed that the interactions of calcium with these five amino acid residues were in the range 2.2–2.5 Å (Harel et al. 2004). In comparison with the aforementioned range, in our glycated model the range was increased to 2.1–5.7 Å for a simulation time of 5 ns (Fig. 6). This difference indicated that the interactive displacement of calcium with five amino acid residues has been increased by glycation. Thus, glycation clearly induces conformational changes in the protein. These findings also predict that the reduced stability may be because of calcium. Table 2 shows the distance of the five key residues from calcium for both glycated and non-glycated huPON1. As is evident from the table, the residues of the non-glycated huPON1 move further away from the calcium at the start of the simulation ($t = 0$ ns) until the end of the simulation ($t = 5$ ns). For the non-glycated huPON1, the greatest movement is that of Glu53 (43.37 Å) and the least is that of Asp269 (23.05 Å), at the end of 5 ns of simulation. For the glycated huPON1, the greatest distance is that of Asn168 (11.14 Å). Interestingly, His115 is closer to the calcium (3.86 Å) at the end of the simulation. Overall, the stability of calcium is compromised because of displacement of calcium at the binding site. The differences between the distances moved by the residues in non-glycated and glycated huPON1 could possibly be attributed to structural constraints imposed on the glycated huPON1. The conformational changes caused by glycation might have prevented key interactions of the residues with the calcium.

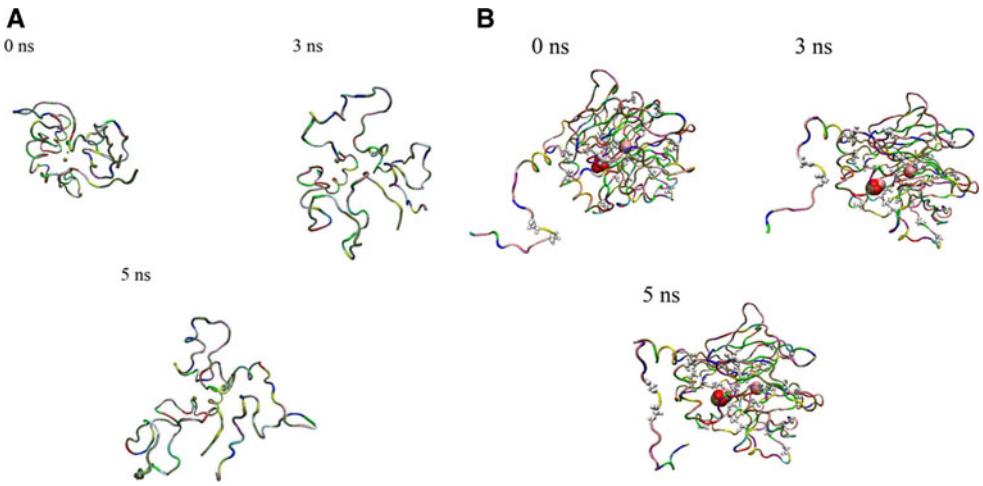

Fig. 5 Schematic diagrams of non-glycated huPON1 (**a**) and pentosidine-glycated huPON1 (**b**) after simulation for 0, 3, and 5 ns

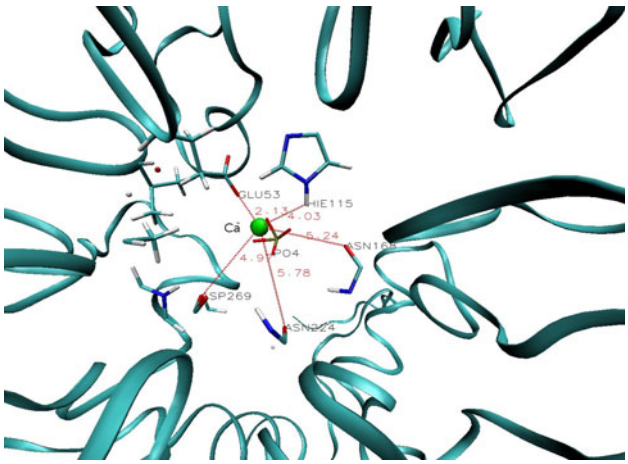

Fig. 6 Conformation of huPON1 (pentosidine-glycated model) observed in MD simulations of the interactions of the catalytic calcium with surrounding residues after 5 ns

Table 2 Distance of key residues from calcium for pentosidine glycated and non-glycated models of huPON1

Time (ns)	Distance of residues from calcium (Å)				
	Type	Glu53	His115	Asn168	Asn224
0	Glycated	5.58	4.91	9.33	6.87
	Non-glycated	5.5	5.06	6	3.7
3	Glycated	6.55	4.17	10.07	8.4
	Non-glycated	20.34	15.8	11.98	13.29
5	Glycated	7.31	3.86	11.14	10.75
	Non-glycated	43.37	27.26	31.15	26.06

Conclusions

This study provides information about the architecture of the active site of huPON1 and about its binding with its substrate. The 3D structures of non-glycated and glycated huPON1 were constructed by homology modeling and the substrate interactions were observed by docking. These investigations suggest the importance of the His115–His134 dyad in both the lactonase and paraoxonase activity of huPON1. Docking output is indicative of hydrogen-bonding interaction of His115 with lactones and paraoxon, whereas Tyr71 and Phe222 participate in hydrophobic interactions. Upon glycation at Lys70 and Lys75, crucial residues undergo conformational variation, resulting in highly disturbed substrate–active site interactions. The residue in the active site lid and Tyr71 interacted weakly with the substrate. This outcome is strongly supported by the MD simulation studies. RMSD and RMSF values for the glycated model are clearly indicative of structural alteration of the protein molecule. Calcium, which is important in the function and stability of the protein, interacts weakly with its surroundings in the glycated model. Calcium seems to be involved in providing structural stability only in its vicinity, and glycation induced conformational changes in the protein throughout the entire simulation. This work has added a new dimension to understanding of and comparison of calcium dynamics in a variety of biological and pharmacological systems.

Acknowledgments Financial support provided by Higher Education Commission, Pakistan, (grant no. 20-752) is gratefully acknowledged. The authors are grateful to David M. Case and his team for providing the license for the Amber 10 software.

References

Altschul SF, Adden TL, Schäffer AA, Zhang J, Zhang Z, Miller W, Lipman DJ (1997) Gapped BLAST and PSI-BLAST: a new generation of protein database search programs. Nucleic Acids Res 25:3389–3402. doi:10.1093/nar/25.17.3389

Azam SS, Hofer TS, Randolf BR, Rode BM (2009) Hydration of sodium(I) and potassium(I) revisited: a comparative QM/MM

and QMCF MD simulation study of weakly hydrated ions. J Phys Chem A 113:1827–1834. doi:10.1021/jp8093462

Bairoch A, Apweiler R (1996) The SWISS-PROT protein sequence data bank and its new supplement TREMBL. Nucleic Acids Res 24:21–25. doi:10.1093/nar/24.1.21

Baynes JW, Thorpe SR (1999) Role of oxidative stress in diabetic complications: a new perspective on an old paradigm. Diabetes 48:1–9. doi:10.2337/diabetes.48.1.1

Berendsen HC, Postma JPM, van Gunsteren WF, Dinola A, Haak JR (1984) Molecular dynamics with coupling to an external bath. J Chem Phys 81:3684–3690. doi:10.1063/1.448118

Billecke S, Draganov D, Counsell R, Stetson P, Watson C, Hsu C, La Du BN (2000) Human serum paraoxonase (pon1) isozymes Q and R hydrolyze lactones and cyclic carbonate esters. Drug Metab Dispos 28:1335–1342

Broomfield CA, Ford KW (1991) Hydrolysis of nerve gases by plasma enzymes. In: Proceedings of the 3rd international meeting on cholinesterases La Grande-Motte France, pp 161

Case DA et al (2008) AMBER 10. University of California, San Francisco

Davies HG, Richter RJ, Keifer M, Broomfield CA, Sowalla J, Furlong CE (1996) The effect of the human serum paraoxonase polymorphism is reversed with diazoxon, soman and sarin. Nat Genet 14:334–336. doi:10.1038/ng1196-334

Dhalla NS, Temsah RM, Netticadan T (2000) Role of oxidative stress in cardiovascular diseases. J Hypertens 18:655–673. doi:10.1097/00004872-200018060-00002

Eckerson HW, Swendris R, Smolen A, La Du BN (1982) A quantitative analysis of the calcium requirement of the human serum paraoxonase/arylesterase. Pharmacologist 24:232

Gohlke H, Hendlich M, Klebe G (2000) Knowledge-based scoring function to predict protein-ligand interactions. J Mol Biol 295:337–356. doi:10.1006/jmbi.1999.3371

Harel M, Aharoni A, Gaidukov L, Brumshtein B, Khersonsky O, Meged R, Dvir H, Ravelli RB, McCarthy A, Toker L, Silman I, Sussman JL, Tawfik DS (2004) Structure and evolution of the serum paraoxonase family of detoxifying and anti-atherosclerotic enzymes. Nat Struct Mol Biol 11:412–419. doi:10.1038/nsmb767

Hashim Z, Zarina S (2007) Assessment of paraoxonase activity and lipid peroxidation levels in diabetic and senile subjects suffering from cataract. Clin Biochem 40:705–709. doi:10.1016/j.clinbiochem.2007.03.015

Hashim Z, Ilyas A, Saleem A, Salim A, Zarina S (2009) Expression and activity of paraoxonase 1 in human cataractous lens tissue. Free Radic Biol Med 46:1089–1095. doi:10.1016/j.freeradbiomed.2009.01.012

Hedrick CC, Thorpe SR, Fu MX, Harper CM, Yoo J, Kim SM, Wong H, Peters AL (2000) Glycation impairs high-density lipoprotein function. Diabetologia 43:312–320. doi:10.1007/s001250050049

Hu X, Jiang X, Lenz DE, Cerasoli MD, Wallqvist A (2009) In silico analyses of substrate interactions with human serum paraoxonase 1. Proteins 75:486–498. doi:10.1002/prot.22264

Humphrey W, Dalke A, Schulten K (1996) VMD: visual molecular dynamics. J Mol Graph 14:33–38. doi:10.1016/0263-7855(96)00018-5

Josse D, Lockridge O, Xie W, Bartels CF, Schopfer LM, Masson P (2001) The active site of human paraoxonase (PON1). J Appl Toxicol 21:7–11. doi:10.1002/jat.789

Khersonsky O, Tawfik SD (2006) The histidine 115-histidine 134 dyad mediates the lactonase activity of mammalian serum paraoxonases. J Biol Chem 281:7649–7656. doi:10.1074/jbc.M512594200

Kramer B, Rarey M, Lengauer T (1999) Evaluation of the FLEXX incremental construction algorithm for protein-ligand docking. Proteins 37:228–241. doi:10.1002/(SICI)1097-0134(19991101)37:2<228:AID-PROT8>3.0.CO;2-8

Kuo CL, La Du BN (1995) Comparison of purified human and rabbit serum paraoxonases. Drug Metab Dispos 23:935–944

Kuo CL, La Du BN (1998) Calcium binding by human and rabbit serum paraoxonases. Structural stability and enzymatic activity. Drug Metab Dispos 26:653–660

Laskowski RA, MacArthur MW, Moss DS, Thornton JM (1993) PROCHECK: a program to check the stereochemical quality of protein structures. J Appl Crystallogr 26:283–291. doi:10.1107/S0021889892009944

Liu Y, Mackness B, Mackness M (2008) Comparison of the ability of paraoxonases 1 and 3 to attenuate the in vitro oxidation of low-density lipoprotein and reduce macrophage oxidative stress. Free Radic Biol Med 45:743–748. doi:10.1016/j.freeradbiomed.2008.05.024

Lu YS, Jiang JY, Lv J, Wu XT, Yu SQ, Zhu WL (2010) Molecular docking and molecular dynamics simulation studies of GPR40 receptor-agonist interactions. Mol Graph Model 28:766–774. doi:10.1016/j.jmgm.2010.02.001

Mackness MI (1989) Possible medical significance of human serum 'A'- esterases. In: Reiner E, Aldridge WN, Hoskin FCG (eds) Enzymes hydrolysing organophosphorus compounds. Ellis Horwood Ltd Publishers, Chichester, pp 202–213

Ng CJ, Wadleigh DJ, Gangopadhyay A, Hama S, Grijalva VR, Navab M, Foqelman AM, Reddy ST (2001) Paraoxonase-2 is a ubiquitously expressed protein with antioxidant properties and is capable of preventing cell-mediated oxidative modification of low density lipoprotein. J Biol Chem 276:44444–44449. doi:10.1074/jbc.M105660200

Pettersen EF, Goddard TD, Huang CC, Couch GS, Greenblatt DM et al (2004) UCSF Chimera-a visualization system for exploratory research and analysis. J Comput Chem 25:1605–1612. doi:10.1002/jcc.20084

Primo-Parmo SL, Sorenson RC, Teiber J, La Du BN (1996) The human serum paraoxonase/arylesterase gene (PON1) is one member of a multigene family. Genomics 33:498–507. doi:10.1006/geno.1996.0225

Rarey M, Kramer B, Lengauer T, Klebe G (1996) A fast flexible docking method using an incremental construction algorithm. J Mol Biol 261:470–489. doi:10.1006/jmbi.1996.0477

Reddy ST, Wadleigh DJ, Grijalva V, Ng C, Hama S, Ganqopadhyay A, Shih DM, Lusis AJ, Navab M, Foqelman AM (2001) Human paraoxonase-3 is an HDL-associated enzyme with biological activity similar to paraoxonase-1 protein but is not regulated by oxidized lipids. Arterioscler Thromb Vasc Biol 21:542–547. doi:10.1161/01.ATV.21.4.542

Ryckaert JP, Ciccotti G, Berendsen JC (1977) Numerical integration of the cartesian equations of motion of a system with constraints: molecular dynamics of *n*-alkanes. J Compu Phys 23:327–341. doi:10.1016/0021-9991(77)90098-5

Sali A, Blundell TL (1993) Comparative protein modelling by satisfaction of spatial restraints. J Mol Biol 234:779–815. doi:10.1006/jmbi.1993.1626

Shih DM, Gu L, Xia LYR, Navab M, Li WF, Hama S, Castellani LW, Furlong CE, Costa LG, Foqelman AM, Lusis AJ (1998) Mice lacking serum paraoxonase are susceptible to organophosphate toxicity and atherosclerosis. Nature 394:284–287. doi:10.1038/28406

Upham BL, Wagner JG (2001) Toxicant-induced oxidative stress in cancer. Toxicol Sci 64:1–3

Vinson JA (2006) Oxidative stress in cataracts. Pathophysiology 13:151–162. doi:10.1016/j.pathophys.2006.05.006

Wallace AC, Laskowski RA, Thornton JM (1995) LIGPLOT: a program to generate schematic diagrams of protein-ligand interactions. Prot Eng 8:127–134. doi:10.1093/protein/8.2.127

Wiederstein M, Sippl MJ (2007) ProSA-web: interactive web service for the recognition of errors in three-dimensional structures of proteins. Nucleic Acids Res 35(Suppl 2):W407–W410. doi:10.1093/nar/gkm290